

# Coordination Framework Hosts Consisting of 4-Pyridyl-Substituted Carboxylic Acid (PCA) Dimers and 1D Chains of Ni<sup>2+</sup> and SCN<sup>-</sup>: A Rational Structural Extension toward Coordination Framework Hosts with Large Rectangular Cavities

Ryo Sekiya,\*† Shin-ichi Nishikiori,† and Katsuyuki Ogura‡

Department of Basic Science, Graduate School of Arts and Sciences, The University of Tokyo, 3-8-1 Komaba, Meguro-ku, Tokyo 153-8902, Japan, and Department of Applied Chemistry and Biotechnology, Faculty of Engineering, Chiba University, 1-33 Yayoi-cho, Inage-ku, Chiba 263-8522, Japan

Received March 29, 2006

For the expansion of a rectangular cavity (RC) defined by two isonicotinic acid (isoH) dimers as bridging ligands and two SCN bridges, we conducted a structural extension based on the elongation of the bridging ligands by the replacement of isoH with longer 4-pyridyl-substituted carboxylic acid (PCA). For this purpose, the following three PCAs have been employed: *trans*-3-(4-pyridyl)propenoic acid (acrylH), 4-(4-pyridyl)benzoic acid (pybenH), and *trans*-3-(4-(4-pyridyl)phenyl)propenoic acid (pppeH). Self-assembly of Ni<sup>2+</sup>, SCN<sup>-</sup>, and each of four PCAs involving isoH, acrylH, pybenH, and pppeH in the presence of an aromatic guest gave four inclusion compounds formulated as [Ni(SCN)<sub>2</sub>(isoH)<sub>2</sub>]·1/2(benz[*a*]anthracene) (**1**), [Ni(SCN)<sub>2</sub>(acrylH)<sub>2</sub>]·1/2(benz[*a*]anthracene) (**2**), [Ni(SCN)<sub>2</sub>(pybenH)<sub>2</sub>]·(pyrene) (**3**), and [Ni(SCN)<sub>2</sub>(pppeH)<sub>2</sub>]<sub>3/2</sub>·(benz[*a*]anthracene) (**4**). X-ray crystal structural determination of **1–4** revealed that the proposed structural extension was successful. Their crystal structures are layered structures of two-dimensional (2D) grid-type coordination frameworks (2D host layers) framed with bridging ligands of the corresponding PCA dimers and 1D chains consisting of Ni<sup>2+</sup> ions and μ<sub>1,3</sub>-SCN<sup>-</sup> ions. The lengths of the PCA dimers are 12.269(5) Å (isoH dimer), 16.890(4) Å (acrylH dimer), 20.89(2) Å (pybenH dimer), 25.387(3) Å (pppeH dimer A), and 25.527(4) Å (pppeH dimer B). Each 2D host layer has RCs defined by the two corresponding PCA dimers and the two SCN bridges. The dimensions of RCs are expanded in proportion to the increase in the lengths of the PCA dimers: 29.52 × 5.60–7.20 Å<sup>2</sup> (**4**) > 24.95 × 5.46–7.38 Å<sup>2</sup> (**3**) > 20.88 × 5.49–7.25 Å<sup>2</sup> (**2**) > 16.41 × 5.53–7.43 Å<sup>2</sup> (**1**). These expansions reflect the number of aromatic guests that can be included in RCs. RC of **1** include only one molecule of benz[*a*]anthracene, whereas RCs of **3** or **4** includes two molecules of pyrene or benz[*a*]anthracene, respectively. Comparison of the lengths between the PCA dimers and 4,4'-bipyridine-type ligands demonstrated that a design strategy—the preparation of a bridging ligand through self-assembly of two PCAs—is both efficient and particularly suitable for the preparation of very long bridging ligands.

## Introduction

Self-assembly of two components with the assistance of highly directional and strong non-covalent interaction gives the corresponding homodimer, which is a supramolecular analogue of a single molecule with almost identical molecular structure. The carboxyl functional group has been most frequently employed as a connecting unit of two components

because of its strong propensity for the formation of highly directional and relatively strong hydrogen bonding with its counterpart.<sup>1–3</sup> This propensity originates from self-complementary pairwise O–H/O hydrogen bonding, denoted by R<sub>2</sub><sup>2</sup>(8) graph set<sup>4</sup>, and a substantially large Δ*H* of formation compared with single hydrogen bonding.<sup>1,5</sup> A well-known example of this structural equivalence is a benzoic acid dimer and *p*-terphenyl.<sup>6</sup> As shown in Figure 1, the benzoic acid dimer is a supramolecular analogue of *p*-terphenyl because

\* To whom correspondence should be addressed. Phone: 81-3-5454-6569. Fax: 81-3-5454-6569. E-mail: csekiya@mail.ecc.u-tokyo.ac.jp.

† The University of Tokyo.

‡ Chiba University.

(1) Jeffery, G. A. *An Introduction To Hydrogen Bonding*; Oxford University Press: New York, 1997.

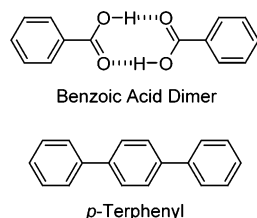
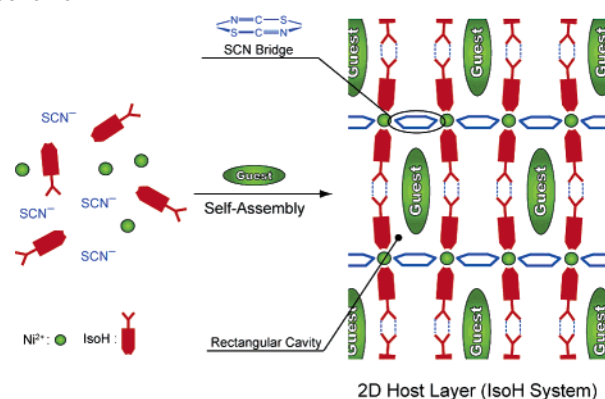


Figure 1.

of the structural equivalence between the  $R_2(8)$  ring system of the benzoic acid dimer and the 1,4-disubstituted phenyl ring of *p*-terphenyl.

From a structural perspective, this equivalence means that carboxylic acid dimers (CADs) can be substituted for their single molecular counterparts. This design strategy is particularly advantageous when their single molecular counterparts have so long and/or large molecular structures that they exhibit poor solubility toward organic solvents and/or water. (Poor solubility originates mainly from their large molecular weight and extensive molecular surface, which strengthen intermolecular interaction, e.g., van der Waals interaction, between molecules and prevent themselves from dissolving into solvents.) A recent work reported by Nangia and co-workers demonstrated the usefulness of this design strategy with 4-(triphenylmethyl)benzoic acid.<sup>7</sup> In that study, they employed this monocarboxylic acid on the basis of notions that (1) its corresponding CAD acts as a supramolecular analogue of 4,4''-bis(triphenylmethyl)-*p*-terphenyl, a wheel-and-axle class of a host compound,<sup>8</sup> and (2) 4,4''-bis(triphenylmethyl)-*p*-terphenyl is expected to exhibit low solubility toward organic solvents originating from its polyaromatic backbone. Indeed, 4-(triphenylmethyl)benzoic

Scheme 1



acid self-assembles to form the corresponding CAD acting as a wheel-and-axle host compound. The resulting CAD forms inclusion compounds with several aromatic solvents.

Our design strategy is to employ CAD as a bridging ligand of a metal–organic coordination framework.<sup>9</sup> The motivation to this is based on the following backgrounds. (1) Most of bridging ligands employed in metal–organic coordination frameworks are single molecules,<sup>10</sup> and thus the employment of CAD as a bridging ligand is of structural interest. (2) Inclusion of large organic molecules requires large cavities whose size must be larger than those of target guests, and thus long bridging ligands, e.g., long 4,4'-bipyridine-type ligands, are required. However, because of the reason mentioned above, such ligands are estimated to exhibit poor solubility toward organic solvents and/or water. Recently, we reported new inclusion compounds characterized by isonicotinic acid (isoH) dimer as a bridging ligands (isoH system).<sup>9</sup> In that study, we successfully exemplified that self-assembly of small components of isoH,  $Ni^{2+}$ , and  $SCN^-$  in the presence of an aromatic guest gives a two-dimensional (2D) grid-type coordination framework (2D host layer), with relatively large rectangular cavities (RCs) defined by two isoH dimers and two  $SCN^-$  bridges, as schematically shown in Scheme 1. In that structure, the isoH dimers act as bridging ligands with more than 12 Å in length, being a supramolecular analogue of a 4,4'-bipyridine-type ligand of 1,4-bis-(4-pyridyl)benzene. The employment of an ambidentate anionic ligand of  $SCN^-$  is based on both prevention of an interpenetrating network by shortening the width of the RC and cancellation of positive charge on metal centers.

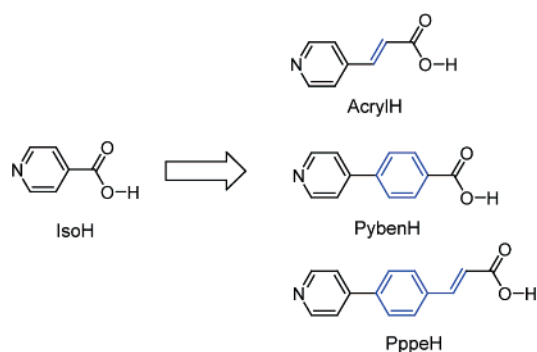
The fact that the dimension of the RC is defined by the length of the isoH dimer led us to anticipate that the replacement of isoH with a longer 4-pyridyl-substituted carboxylic acid (PCA), a structural analogue of isoH, would expand its dimension. For this purpose, we have employed the following three PCAs: *trans*-3-(4-pyridyl)propenoic acid (acrylH), 4-(4-pyridyl)benzoic acid (pybenH), and *trans*-3-(4-(4-pyridyl)phenyl)propenoic acid (pppeH), as shown in

- (2) For recent articles see: (a) George, S.; Goldberg, I. *Cryst. Growth Des.* **2006**, *6*, 755–762. (b) Jayaraman, A.; Balasubramanian, B.; Valiyaveetil, S. *Cryst. Growth Des.* **2004**, *4*, 1403–1409. (c) Gdaniec, M.; Jankowski, W.; Milewska, M. J.; Połoński, T. *Angew. Chem., Int. Ed.* **2003**, *42*, 3903–3906. (d) Qin, Z.; Jennings, M. C.; Puddephatt, R. J. *Inorg. Chem.* **2002**, *41*, 5174–5186. (e) Tang, G.; Zhu, H.-G.; Liang, B.-H.; Chen, X.-M. *J. Chem. Soc., Dalton Trans.* **2001**, 580–585. (f) Gianneschi, N. C.; Tiekink, E. R. T.; Rendina, L. M. *J. Am. Chem. Soc.* **2000**, *122*, 8474–8479. (g) Kolotuchin, S. V.; Thiessen, P. A.; Fenlon, E. E.; Wilson, S. R.; Loweth, C. J.; Zimmerman, S. C. *Chem–Eur. J.* **1999**, *5*, 2537–2547. (h) Holý, P.; Závada, J.; Čísarová, I.; Podlaha, J. *Angew. Chem., Int. Ed.* **1999**, *38*, 381–383. (i) Beketov, K.; Weber, E.; Seidel, J.; Köhnke, K.; Makhkamov, K.; Ibragimov, B. *Chem. Commun.* **1999**, 91–92. (j) Aakeröy, C. B.; Beatty, A. M.; Leinen, D. S. *Angew. Chem., Int. Ed.* **1999**, *38*, 1815–1819. (k) Ashton, P. R.; Collins, A. N.; Fyfe, M. C. T.; Menzer, S.; Stoddart, J. F.; Williams, D. J. *Angew. Chem., Int. Ed.* **1998**, *36*, 735–739.
- (3) For reviews see: (a) Braga, D.; Maini, L.; Polito, M.; Tagliavini, E.; Grepioni, F. *Coord. Chem. Rev.* **2003**, *246*, 53–71. (b) Beatty, A. M. *Coord. Chem. Rev.* **2003**, *246*, 131–143. (c) Braga, D.; Grepioni, F.; Desiraju, G. R. *Chem. Rev.* **1998**, *98*, 1375–1405. (d) Braga, D.; Grepioni, F.; Sabatino, P.; Desiraju, G. R. *Organometallics* **1994**, *13*, 3532–3543. (e) Leiserowitz, L. *Acta Crystallogr., Sect. B* **1976**, *32*, 775–802.
- (4) (a) Bernstein, J.; Davis, R. E.; Shimon, L.; Chang, N.-L. *Angew. Chem., Int. Ed.* **1995**, *34*, 1555–1573. (b) Etter, M. C. *Acc. Chem. Res.* **1990**, *23*, 120–126.
- (5) Gavezzoti, A.; Filippini, G. *J. Phys. Chem.* **1994**, *98*, 4831–4837.
- (6) (a) Desiraju, G. R. *Chem. Commun.* **1997**, 1475–1482. (b) Desiraju, G. R. *Angew. Chem., Int. Ed.* **1995**, *34*, 2311–2327.
- (7) Jetti, R. K. R.; Xue, F.; Mak, T. C. W.; Nangia, A. *J. Chem. Soc., Perkin Trans. 2* **2000**, 1223–1232.
- (8) Toda, F. In *Comprehensive Supramolecular Chemistry*; MacNicol, D. D., Toda, F., Bishio, R., Eds.; Pergamon: Oxford, U.K., 1996; Vol. 6, pp 305–350.

(9) Sekiya, R.; Nishikiori, S.; Ogura, K. *J. Am. Chem. Soc.* **2004**, *126*, 16587–16600.

(10) For reviews see: (a) Kitagawa, S.; Kitaura, R.; Noro, S. *Angew. Chem., Int. Ed.* **2004**, *43*, 2334–2375. (b) Eddaoudi, M.; Moler, D. B.; Li, H.; Chen, B.; Reineke, T. M.; O'Keeffe, M.; Yaghi, O. M. *Acc. Chem. Res.* **2001**, *34*, 319–330. (c) Zaworotko, M. J. *Chem. Commun.* **2001**, 1–9.

## Scheme 2



Scheme 2. Their corresponding CADs can act as very long bridging ligands, some of which are more than 20 Å in length. Self-assembly of Ni<sup>2+</sup>, SCN<sup>-</sup>, and each of three PCAs would result in the formation of 2D host layers whose fundamental architectures are almost identical to that of the starting host system but have expanded RCs. In principle, resulting RCs would include much larger molecules that cannot be included in RC of the isoH system and the number of the guests that can be included in the resulting RCs would increase two or more. Therefore, the proposed structural extension is a fundamental and important investigation aimed at the construction of new host systems.

In the present study, we will describe a successful structural extension from the isoH system and the usefulness of our design strategy through both introduction of four inclusion compounds and comparison of the resulting PCA dimers with 4,4'-bipyridine-type ligands employed in metal-organic coordination frameworks. The four inclusion compounds reported herein are [Ni(SCN)<sub>2</sub>(isoH)<sub>2</sub>]·1/2(benz[*a*]anthracene) (**1**) (isoH system), [Ni(SCN)<sub>2</sub>(acrylH)<sub>2</sub>]·1/2(benz[*a*]anthracene) (**2**) (acrylH system), [Ni(SCN)<sub>2</sub>(pybenH)<sub>2</sub>]·(pyrene) (**3**) (pybenH system), and [Ni(SCN)<sub>2</sub>(pppeH)<sub>2</sub>]·3/2(benz[*a*]anthracene) (**4**) (pppeH system).

## Experimental Section

**General Methods.** Unless stated otherwise, reagents and solvents were purchased from commercial sources and used directly. Synthesis of pybenH, *trans*-4-(2-carboxyethenyl)benzeneboronic acid, and pppeH was conducted under a dry nitrogen atmosphere. Melting points were determined using a Laboratory Devices Inc. melting point apparatus and are uncorrected. <sup>1</sup>H NMR spectra and <sup>13</sup>C NMR spectra were recorded on a JEOL α-500. All infrared spectra were measured on a JASCO FT/IR-350 spectrometer by the KBr disk method at room temperature. Mass spectra were measured on a JEOL JMS-600H machine under electron impact at 70 eV.

**Synthesis. 4-(4-Pyridyl)benzoic Acid (pybenH).**<sup>11</sup> Pd(PPh<sub>3</sub>)<sub>4</sub> (0.30 g, 0.26 mmol) was added to a degassed solution of carboxybenzene boronic acid (1.70 g, 10.2 mmol), 4-bromopyridine hydrochloride (2.01 g, 10.3 mmol), and sodium carbonate (2.10 g, 19.8 mmol) in 120 mL of a mixed solution (1:1 CH<sub>3</sub>CN:H<sub>2</sub>O) at 25 °C. The mixture was refluxed under N<sub>2</sub> for 22 h. The hot suspension was filtered. The filtrate was concentrated to about half of the original volume and then washed with CH<sub>2</sub>Cl<sub>2</sub>. The aqueous

layer was acidified with concentrated HCl; the resulting white precipitate was collected, washed with CH<sub>3</sub>CN, and recrystallized from pyridine to afford 4-(4-pyridyl)benzoic acid (1.72 g, 8.63 mmol) in 85% yield. Mp: >330 °C (dec). IR (KBr, ν<sub>max</sub>): 2431, 1700, 1604, 1403, 1317, 1296, 1180, 1073, 1006, 828, 733, 742, 701, 668, 519 cm<sup>-1</sup>. <sup>1</sup>H NMR (DMSO-*d*<sub>6</sub>, 500 MHz): δ 13.13 (br. s, 1H), 8.67 (dd, 2H, 1.53 Hz, 4.57 Hz), 8.06 (dd, 2H, 1.83 Hz, 6.72 Hz), 7.92 (dd, 2H, 1.83 Hz, 6.72 Hz), 7.76 (dd, 2H, 1.53 Hz, 4.57 Hz). <sup>13</sup>C NMR (DMSO-*d*<sub>6</sub>, 126 MHz): δ 166.90, 150.33, 145.96, 141.24, 131.26, 130.08, 127.11, 121.46. MS (EI, 70 eV, *m/z*): 199 (M<sup>+</sup>), 182 (OH), 154 (CO<sub>2</sub>H). Anal. Calcd for C<sub>12</sub>H<sub>9</sub>NO<sub>2</sub>: C, 72.35; H, 4.55; N, 7.03. Found: C, 72.26; H, 4.58; N, 6.83.

***trans*-4-(2-Carboxyethenyl)benzeneboronic Acid.** Malonic acid (0.72 g, 6.92 mmol) was added to a degassed solution of *p*-formylbenzeneboronic acid (0.50 g, 3.33 mmol) in 30 mL of pyridine at 25 °C and 0.1 cm<sup>3</sup> of piperidine was then added to the solution. The mixture was refluxed under N<sub>2</sub> for 13 h. The solvent was removed under reduced pressure. The residue was taken up in water that was acidified with concentrated HCl; the resulting white precipitate was collected, washed with water, and dried under reduced pressure to afford *trans*-4-(2-carboxyethenyl)benzeneboronic acid (0.59 g, 3.07 mmol) in 92% yield. Mp: 194–195 °C. IR (KBr, ν<sub>max</sub>): 3346, 2518, 1659, 1511, 1411, 1339, 1311, 1268, 1151, 1061, 975, 876, 786, 676 cm<sup>-1</sup>. <sup>1</sup>H NMR (DMSO-*d*<sub>6</sub>, 500 MHz) δ 12.42 (br. s, 1H), 8.16 (br. s, 2H), 7.80 (d, 2H, 8.09 Hz), 7.62 (d, 2H, 8.09 Hz), 7.57 (d, 2H, 16.17 Hz), 6.54 (d, 2H, 16.17 Hz). <sup>13</sup>C NMR (DMSO-*d*<sub>6</sub>, 126 MHz) δ 167.61, 143.87, 136.39, 135.61, 134.55, 127.14, 119.67. MS (EI, 70 eV, *m/z*): 147 (-B(OH)<sub>2</sub>), 131, (-B(OH)<sub>2</sub>, -OH), 103 (-B(OH)<sub>2</sub>, -CO<sub>2</sub>H). Anal. Calcd for C<sub>9</sub>H<sub>9</sub>BO<sub>4</sub>: C, 56.31; H, 4.72. Found: C, 56.07; H, 4.82.

***trans*-3-(4-(4-Pyridyl)phenyl)propenoic Acid (pppeH).** Pd(PPh<sub>3</sub>)<sub>4</sub> (61 mg, 5.3 × 10<sup>-2</sup> mmol) was added to a degassed solution of (*E*)-4-(2-carboxylethenyl)benzeneboronic acid (1.02 g, 5.31 mmol), 4-bromopyridine hydrochloride (1.05 g, 5.40 mmol), and sodium carbonate (1.82 g, 17.2 mmol) in 80 mL of a mixed solution (1:1 CH<sub>3</sub>CN; H<sub>2</sub>O) at 25 °C. The mixture was refluxed under N<sub>2</sub> for 20 h. The hot suspension was filtered. The filtrate was concentrated to about half of the original volume and then washed with CH<sub>2</sub>Cl<sub>2</sub>. The aqueous layer was acidified with concentrated HCl; the resulting white precipitate was collected, washed with CH<sub>3</sub>CN, and recrystallized from pyridine to afford desired product (0.96 g, 4.26 mmol) in 80% yield. Mp: >330 °C (dec). IR (KBr, ν<sub>max</sub>): 2363, 1923, 1700, 1636, 1605, 1408, 1194, 1064, 1019, 1007, 814, 684, 607, 521, 496 cm<sup>-1</sup>. <sup>1</sup>H NMR (DMSO-*d*<sub>6</sub>, 500 MHz) δ 12.48 (br. s, 1H), 8.64 (dd, 2H, 1.53 Hz, 4.58 Hz), 7.85 (m, 4H), 7.75 (dd, 2H, 1.53 Hz, 4.58 Hz), 7.64 (d, 1H, 16.17 Hz), 6.62 (d, 1H, 16.17 Hz). <sup>13</sup>C NMR (DMSO-*d*<sub>6</sub>, 126 MHz): δ 167.48, 150.30, 146.04, 143.36, 138.51, 135.11, 129.00, 127.27, 121.11, 120.12. MS (EI, 70 eV, *m/z*): 225 (M<sup>+</sup>), 208 (-OH), 180 (-CO<sub>2</sub>H); Anal. Calcd for C<sub>14</sub>H<sub>11</sub>NO<sub>2</sub>: C, 74.65; H, 4.92; N, 6.22. Found: C, 74.55; H, 4.73; N, 6.01.

**[Ni(SCN)<sub>2</sub>(isoH)<sub>2</sub>]·1/2(benz[*a*]anthracene) (**1**).** To an acetonitrile solution (120 mL) in which NiCl<sub>2</sub>·6H<sub>2</sub>O (0.12 g, 0.51 mmol) was suspended was added KSCN (0.10 g, 1.03 mmol) with vigorous stirring, and the mixture was refluxed for 1 h. After the precipitated KCl was filtered off, isonicotinic acid (0.12 g, 0.97 mmol) was added to the solution. The solution was left for 24 h at room temperature, and then benz[*a*]anthracene was added. Green crystals of **1** were obtained after slow evaporation of the solvent over a period of a few weeks at room temperature. The crystals were collected, washed with acetonitrile, and dried in the air. Mp: >330

(11) PybenH was synthesized by a modified procedure based on a literature method. See: Gong, Y.; Pauls, H. W. *Synlett* **2000**, 6, 829–831.



°C (dec). Anal. Calcd for  $C_{23}H_{16}N_4O_4S_2Ni$ : C, 51.61; H, 3.02; N, 10.47. Found: C, 51.59; H, 3.06; N, 10.39.

**[Ni(SCN)<sub>2</sub>(acrylH)<sub>2</sub>·1/2(benz[a]anthracene) (2).** To methanol solution (100 mL) in which  $NiCl_2 \cdot 6H_2O$  (0.18 g, 0.76 mmol) was suspended was added KSCN (0.15 g, 1.54 mmol) was added with vigorous stirring, and the mixture was refluxed for 1 h. After the precipitated KCl was filtered off, *trans*-3-(4-pyridyl)propenoic acid (0.30 g, 1.51 mmol) was added to the solution. The solution was left for 24 h at room temperature, and benz[a]anthracene was then added. Green crystals of **2** were obtained after slow evaporation of the solvent over a period of a few weeks at room temperature. The crystals were collected, washed with methanol, and dried in the air. Mp: >330 °C (dec). Anal. Calcd for  $C_{27}H_{20}N_4O_4S_2Ni$ : C, 55.21; H, 3.41; N, 9.54. Found: C, 55.31; H, 3.51; N, 9.48.

**[Ni(SCN)<sub>2</sub>(pybenH)<sub>2</sub>·(pyrene) (3).** To a methanol solution (200 mL) in which  $NiCl_2 \cdot 6H_2O$  (0.18 g, 0.76 mmol) was suspended was added KSCN (0.15 g, 1.54 mmol) with vigorous stirring, and the mixture was refluxed for 1 h. After the precipitated KCl was filtered off, 4-(4-pyridyl)benzoic acid (0.30 g, 1.51 mmol) was added to the solution. The solution was left for 24 h at room temperature, and pyrene was then added. Green crystals of **3** were obtained after slow evaporation of the solvent over a period of a few weeks at room temperature. The crystals were collected, washed with methanol, and dried in the air. Mp: >330 °C (dec). Anal. Calcd for  $C_{42}H_{28}N_4O_4S_2Ni$ : C, 65.04; H, 3.05; N, 7.23. Found: C, 65.04; H, 3.71; N, 7.06.

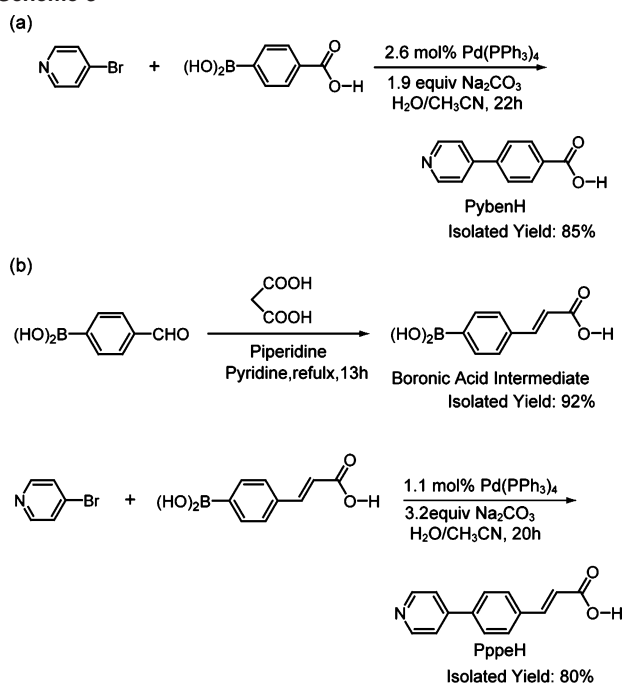
**[Ni(SCN)<sub>2</sub>(pppeH)<sub>2</sub>·3/2·(benz[a]anthracene) (4).** To a methanol solution (100 mL) in which  $NiCl_2 \cdot 6H_2O$  (0.07 g, 0.30 mmol) was suspended was added KSCN (0.06 g, 0.62 mmol) with vigorous stirring, and the mixture was refluxed for 1 h. After the precipitated KCl was filtered off, *trans*-3-(4-(4-pyridyl)phenyl)propenoic acid (0.13 g, 0.58 mmol) was dissolved. The solution was left for 24 h at room temperature, and benz[a]anthracene was then added to the solution. Green crystals of **4** were obtained after slow evaporation of the solvent over a period of a few weeks at room temperature. The crystals were collected, washed with methanol, and dried in the air. Mp: >330 °C (dec). Anal. Calcd for  $C_{63}H_{45}N_6O_6S_3Ni_{1.5}$ : C, 64.88; H, 3.89; N, 7.21. Found: C, 64.68; H, 3.95; N, 7.03.

**X-ray Crystal Structure Determination.** The intensity data of **1–4** were collected on a Rigaku RAXIS–RAPID imaging plate area detector using graphite-monochromatized Mo K $\alpha$  radiation ( $\lambda / \text{Å} = 0.71069$ ). The crystal structures were solved by the direct method using the *SHELXS-97* program<sup>12</sup> and refined by successive differential Fourier syntheses and full-matrix least-squares procedures using the *SHELXL-97* program.<sup>13</sup> Anisotropic thermal factors were applied to all non-hydrogen atoms. All hydrogen atoms were generated geometrically.

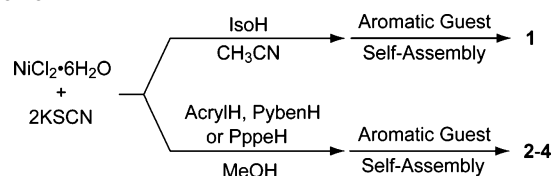
## Synthesis

**Synthesis of Building Blocks.** PybenH<sup>11</sup> and pppeH were synthesized as outlined in Scheme 3. PybenH was synthesized by a Pd-catalyzed cross-coupling reaction of 4-bromopyridine hydrochloride with 4-carboxybenzeneboronic acid in the presence of  $Na_2CO_3$  as base and a catalytic amount of  $Pd(PPh_3)_4$  in 1:1  $CH_3CN:H_2O$  solution in 85% isolated yield. PppeH was synthesized from *p*-formylbenzeneboronic acid in two steps. Knoevenagel condensation of *p*-formylbenzeneboronic acid with malonic acid in the presence of piperidine in pyridine solution provided *trans*-4-(2-carboxyethenyl)benzeneboronic acid (boronic acid intermediate) in

## Scheme 3



## Scheme 4



92% isolated yield. No corresponding *cis*-isomer was obtained. Subsequent Pd-catalyzed cross-coupling reactions of 4-bromopyridine hydrochloride with the boronic acid intermediate in the presence of  $Na_2CO_3$  as base and catalytic amount of  $Pd(PPh_3)_4$  in 1:1  $CH_3CN:H_2O$  solution provided pppeH in 80% isolated yield.

**Preparation of Inclusion Compounds.** Diffraction-quality green crystals of **1** were prepared by slow evaporation at room temperature of an acetonitrile solution containing  $Ni^{2+}$ ,  $SCN^-$ , isoH, and benz[a]anthracene (Scheme 4). Green crystals of **2–4** were prepared from methanol solutions by methods almost identical to that of **1**. IR spectra of **1–4** exhibited strong and sharp peaks characteristic of carboxyl functional group and  $SCN^-$  ion as intermetallic bridge at 1684–1706 and 2101–2120  $cm^{-1}$ , respectively. Broad absorption bands with some weak peaks in the range of 2300–3200  $cm^{-1}$  suggested the formation of hydrogen bonding between the carboxyl functional groups of the corresponding PCAs. The IR spectra of **1–4** are shown in Figures S1–S4, respectively, of the Supporting Information. All inclusion compounds are air-stable and insoluble in common organic solvents except for polar ones such as DMF and DMSO.

**X-ray Crystallography.** X-ray crystal structure determination of **1–4** revealed their compositions to be  $[Ni(SCN)_2(isoH)_2] \cdot 1/2 \cdot (benz[a]anthracene)$ ,  $[Ni(SCN)_2(acrylH)_2] \cdot 1/2 \cdot (benz[a]anthracene)$ ,  $[Ni(SCN)_2(pybenH)_2] \cdot (pyrene)$ , and  $[Ni(SCN)_2(pppeH)_2]_{3/2} \cdot (benz[a]anthracene)$ , respectively. All inclusion compounds belong to the triclinic crystal system with space group  $P\bar{1}$  (No. 2). Detailed crystallographic data and their host:guest ratios (host-to-guest stoichiometric ratios) are listed in Table 1. Neither solvent of crystallization nor counterion was found in the crystal structures of **1–4**. Because the carboxyl hydrogen atoms of PCAs could not be found in difference maps, the hydrogen atoms were placed at

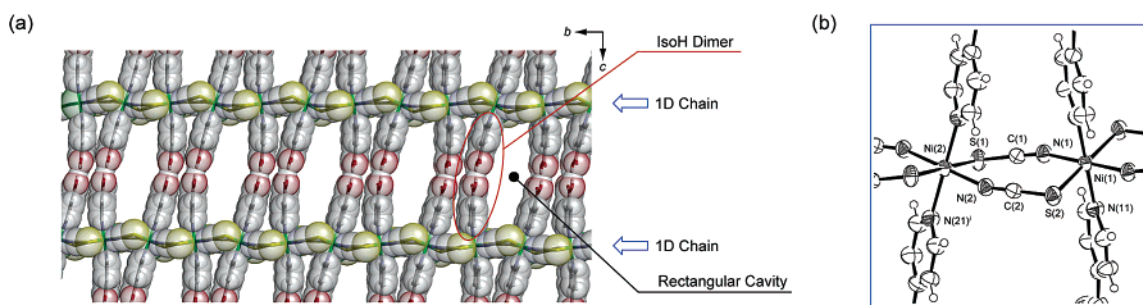
(12) Sheldrick, G. M. *SHELXS-97: Program for X-ray Crystal Structure Refinement*; University of Göttingen: Göttingen, Germany, 1997.

(13) Sheldrick, G. M. *SHELXL-97: Program for the Refinement of Crystal Structures*; University of Göttingen: Göttingen, Germany, 1997.

**Table 1.** Crystallographic Data for the Inclusion Compounds of **1–4**

	<b>1</b>	<b>2</b>	<b>3</b>	<b>4</b>
formula	C <sub>23</sub> H <sub>16</sub> N <sub>4</sub> O <sub>4</sub> S <sub>2</sub> Ni	C <sub>27</sub> H <sub>20</sub> N <sub>4</sub> O <sub>4</sub> S <sub>2</sub> Ni	C <sub>23</sub> H <sub>16</sub> N <sub>4</sub> O <sub>4</sub> S <sub>2</sub> Ni	C <sub>63</sub> H <sub>45</sub> N <sub>6</sub> O <sub>6</sub> S <sub>3</sub> Ni <sub>1.5</sub>
aromatic guest	benz[ <i>a</i> ]anthracene	benz[ <i>a</i> ]anthracene	pyrene	benz[ <i>a</i> ]anthracene
host-to-guest ratio <sup>a</sup>	2:1	2:1	1:1	3:2
fw	535.2	587.3	755.5	1166.3
<i>T</i> (K)	298	123	183	153
cryst syst	triclinic	triclinic	triclinic	triclinic
space group	<i>P</i> 1̄ (No. 2)	<i>P</i> 1̄ (No. 2)	<i>P</i> 1̄ (No. 2)	<i>P</i> 1̄ (No. 2)
<i>a</i> (Å)	10.025(2)	9.7107(8)	10.69(1)	10.9741(4)
<i>b</i> (Å)	11.0678(9)	10.982(1)	10.926(7)	16.7548(4)
<i>c</i> (Å)	17.963(2)	20.646(2)	26.82(2)	33.6402(9)
α (deg)	114.955(7)	95.132(3)	115.63(7)	120.456(3)
β (deg)	50.81(2)	35.560(4)	45.8(1)	37.446(1)
γ (deg)	131.83(1)	90.949(3)	128.98(7)	134.530(5)
<i>V</i> (Å <sup>3</sup> )	1151(3)	1269(1)	1747(9)	2665(2)
<i>Z</i>	2	2	2	2
ρ <sub>calcd</sub> (g cm <sup>-3</sup> )	1.54	1.54	1.47	1.45
μ (Mo Kα) (mm <sup>-1</sup> )	1.063	0.971	0.726	0.714
2θ <sub>max</sub> (deg)	60	60	60	60
no. of refls obsd <sup>b</sup>	5997	6827	8683	15107
no. of refls used <sup>c</sup>	3910	4388	2332	9608
params	391	427	481	799
R1 <sup>d</sup>	0.0663	0.0608	0.0695	0.0484
wR2 <sup>e</sup>	0.1745	0.1712	0.2083	0.1309
GOF	1.103	1.000	0.782	0.957

<sup>a</sup> Host-to-guest stoichiometric ratio. <sup>b</sup> The number of observed reflections. <sup>c</sup> The number of reflections used in the structure determination. <sup>d</sup> R1 = (Σ||*F*<sub>o</sub> - |*F*<sub>c</sub>||)/Σ|*F*<sub>o</sub>|. <sup>e</sup> wR2 = [(Σ(w(*F*<sub>o</sub><sup>2</sup> - *F*<sub>c</sub><sup>2</sup>))/Σ(w(*F*<sub>o</sub><sup>2</sup>))]<sup>1/2</sup>.



**Figure 2.** (a) Framework with van der Waals surface of the 2D host layer of **1** spreading over the *bc* plane. Benz[*a*]anthracene guests are omitted for clarity. Color scheme: gray (carbon), white (hydrogen), blue (nitrogen), red (oxygen), yellow (sulfur). (b) Coordination environment around Ni(1) and Ni(2) in **1** (50% probability level ellipsoids). Symmetry code used to generate equivalent atoms: (i) - *x*, 1 - *y*, 1 - *z*.

calculated positions adjacent to the oxygen atom with the longer carbon-to-oxygen bond length.

In the following crystal structure descriptions, axis settings are used for easy structural comparison among **1–4**. 1D chains propagate along the *b* axis. Ni<sup>2+</sup>–PCA/PCA–Ni<sup>2+</sup> linkages propagate along the [012] axis for **1–3** and the [023] axis for **4**. Two-dimensional host layers spread over the *bc* plane and are stacked parallel to the *bc* plane.

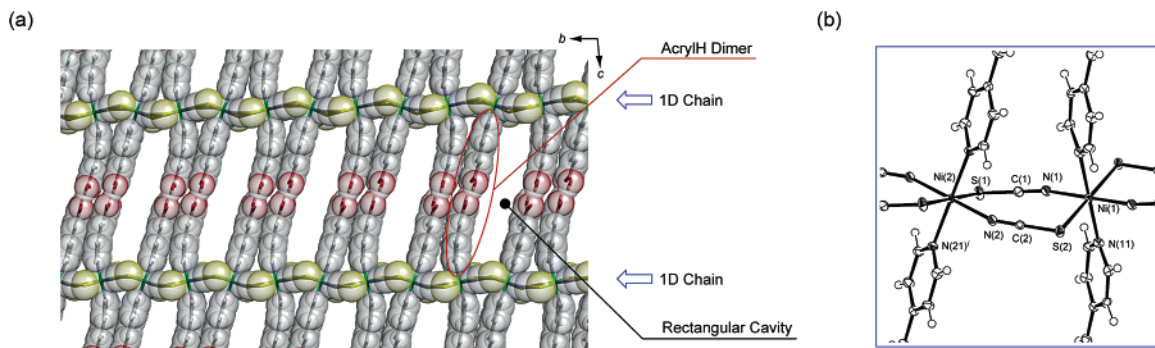
### Description of the Crystal Structures

**General.** The crystal structures of **1–4** are characterized by layered structures of 2D host layers composed of Ni<sup>2+</sup>, SCN<sup>-</sup>, and the corresponding PCA ligands. Their architectures are generally identical to each other. However, some differences were found between **4** and the others. Thus, we will describe first the structure of the 2D host layer of **3**, as a representative of **1–3**, and then that of the 2D host layer of **4**. After that, we will describe the crystal structures of **1–4**.

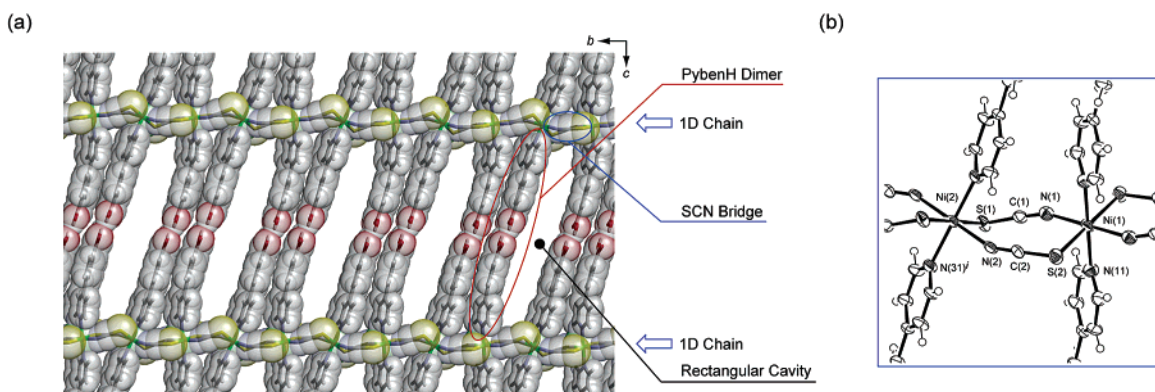
**Architecture of the 2D Host Layer of 3.** The coordination framework with van der Waals surface of the 2D host layer formed in **3** and the ORTEP drawing of the coordination

environments around metal centers with a major atom numbering scheme are shown in panels a<sup>14</sup> and b of Figure 4, respectively. (The corresponding coordination frameworks and coordination environments of **1** and **2** are shown in Figures 2 and 3, respectively.) The asymmetric unit contains two Ni<sup>2+</sup> ions (Ni(1) and Ni(2)) with octahedral coordination geometries, two SCN<sup>-</sup> ions, two pybenH ligands, and a pyrene guest. (The asymmetric units of **1** and **2** contain half of a benz[*a*]anthracene guest.) The Ni<sup>2+</sup> ions lie on crystallographic inversion centers. Figure 4b shows that four equatorial coordination sites of each Ni<sup>2+</sup> ion are occupied by two nitrogen atoms from SCN<sup>-</sup> ions and two sulfur atoms from SCN<sup>-</sup> ions in trans configurations. The SCN<sup>-</sup> ions act as μ<sub>1,3</sub>-intermetallic bridges and doubly connect adjacent Ni<sup>2+</sup> ions in antiparallel fashion with an Ni(1)/Ni(2) separation of 5.5643(3) Å to build up an 1D chain propagating along the *b* axis. (The corresponding Ni/Ni separations found in **1** and **2** are 5.5339(5) and 5.4908(5) Å, respectively.) Two pybenH ligands are bonded to the remaining axial coordina-

(14) Merritt, E. A.; Bacon, D. J. *Raster3D: Photorealistic Molecular Graphics; Methods Enzymol.* **1997**, *277*, 505–524.



**Figure 3.** (a) Framework with van der Waals surface of the 2D host layer of **2** spreading over the  $bc$  plane. Benz[*a*]anthracene guests are omitted for clarity. Color scheme: gray (carbon), white (hydrogen), blue (nitrogen), red (oxygen), yellow (sulfur), green (nickel). (b) The coordination environment around Ni(1) and Ni(2) in **2** (50% probability level ellipsoids). Symmetry code used to generate equivalent atoms: (i)  $-x, 1 - y, 1 - z$ .



**Figure 4.** Framework with van der Waals surface of the 2D host layer of **3** spreading over the  $bc$  plane. Pyrene guests are omitted for clarity. Color scheme: gray (carbon), white (hydrogen), blue (nitrogen), red (oxygen), yellow (sulfur), green (nickel). (b) Coordination environment around Ni(1) and Ni(2) in **3** (50% probability level ellipsoids). Symmetry code used to generate equivalent atoms: (i)  $-x, 1 - y, 1 - z$ .

**Table 2.** Selected Bond Distances (Å) and Angles (deg) for **1**<sup>a</sup>

Ni(1)–N(1)	2.033(4)	Ni(1)–N(11)	2.139(4)
Ni(1)–S(2)	2.516(1)	Ni(2)–N(2)	2.036(3)
Ni(2)–N(21) <sup>i</sup>	2.133(4)	Ni(2)–S(1)	2.530(1)
N(1)–Ni(1)–N(11)	90.7(1)	N(1)–Ni(1)–S(2)	92.5(1)
N(11)–Ni(1)–S(2)	89.6(1)	N(2)–Ni(2)–N(21) <sup>i</sup>	89.7(1)
N(2)–Ni(2)–S(1)	93.9(1)	N(21) <sup>i</sup> –Ni(2)–S(2)	89.1(1)

<sup>a</sup> Symmetry code used to generate equivalent atoms: (i)  $-x, 1 - y, 1 - z$ .

tion sites of each Ni<sup>2+</sup> ion via pyridyl nitrogen atoms. Neither coordination of the carboxyl oxygen of a pybenH ligand to a metal center nor deprotonation of the carboxyl hydrogen from a pybenH ligand was found. Both phenomena are common in other systems where a PCA ligand, in most cases isoH, was employed as a building block.<sup>2i,15</sup> The bond lengths and angles of the coordination spheres of the Ni<sup>2+</sup> ions are compiled in Table 4. (The corresponding bond lengths and angles of **1** and **2** are compiled in Tables 2 and 3, respectively.)

Each pybenH ligand forms a pybenH dimer with a pybenH ligand of an adjacent 1D chain through self-complementary pairwise O–H/O hydrogen bonding ( $R_2^2(8)$  graph set) with O/O distances in the range 2.593(7)–2.661(7) Å, giving rise to the 2D host layer spreading over the  $bc$  plane. (The corresponding O/O distances found in **1** and **2** are in the ranges 2.605(8)–2.654(7) and 2.626(4)–2.623(4) Å, respec-

**Table 3.** Selected Bond Distances (Å) and Angles (deg) for **2**<sup>a</sup>

Ni(1)–N(1)	2.022(3)	Ni(1)–N(11)	2.110(3)
Ni(1)–S(2)	2.5425(9)	Ni(2)–N(2)	2.035(3)
Ni(2)–N(21) <sup>i</sup>	2.116(3)	Ni(2)–S(1)	2.507(1)
N(1)–Ni(1)–N(11)	90.4(1)	N(1)–Ni(1)–S(2)	93.71(9)
N(11)–Ni(1)–S(2)	89.09(8)	N(2)–Ni(2)–N(21) <sup>i</sup>	90.8(1)
N(2)–Ni(2)–S(1)	92.95(9)	N(21) <sup>i</sup> –Ni(2)–S(2)	89.40(8)

<sup>a</sup> Symmetry code used to generate equivalent atoms: (i)  $-x, 1 - y, 1 - z$ .

**Table 4.** Selected Bond Distances (Å) and Angles (deg) for **3**<sup>a</sup>

Ni(1)–N(1)	2.077(7)	Ni(1)–N(11)	2.118(6)
Ni(1)–S(2)	2.515(5)	Ni(2)–N(2)	2.013(7)
Ni(2)–N(31) <sup>i</sup>	2.124(6)	Ni(2)–S(1)	2.587(7)
N(1)–Ni(1)–N(11)	90.6(3)	N(1)–Ni(1)–S(2)	91.1(2)
N(11)–Ni(1)–S(2)	87.3(2)	N(2)–Ni(2)–N(31) <sup>i</sup>	89.5(2)
N(2)–Ni(2)–S(1)	93.4(2)	N(31) <sup>i</sup> –Ni(2)–S(2)	89.6(2)

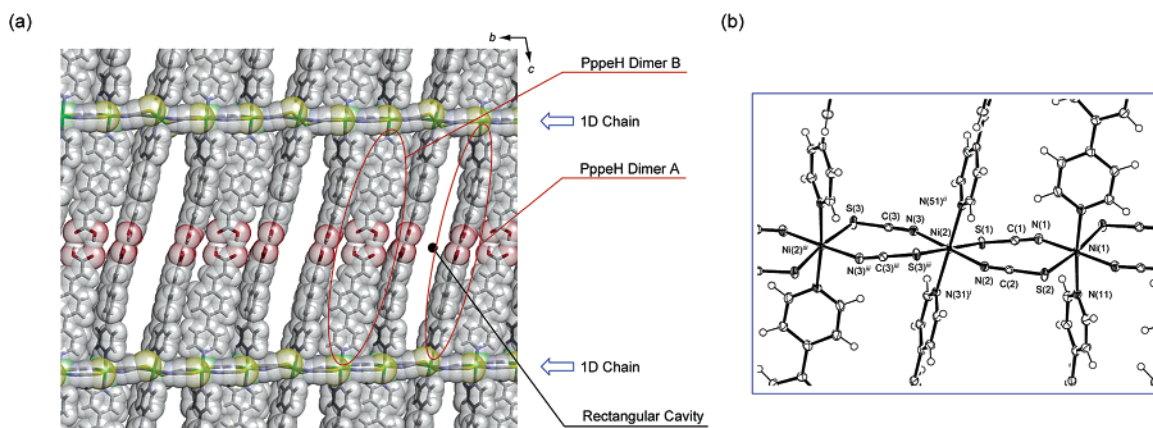
<sup>a</sup> Symmetry code used to generate equivalent atom: (i)  $-x, 1 - y, 1 - z$ .

tively.) The pybenH dimers connect Ni<sup>2+</sup> ions with a Ni/Ni separation of 24.95(2) Å. (The corresponding Ni/Ni separations of **1** and **2** are 16.414(2) and 20.884(2) Å, respectively.) The Ni<sup>2+</sup>–pybenH/pybenH–Ni<sup>2+</sup> linkages propagate along the [012] axis. Figure 4a shows that the 2D host layers have RCs defined by two pybenH dimers and two SCN bridges.

**Architecture of the 2D host layer of 4.** The coordination framework with van der Waals surface of the 2D host layer formed in **4** and the ORTEP drawing of the coordination environments around metal centers with a major atom numbering scheme are shown in panels a<sup>14</sup> and b of Figure

(15) MacGillivray, L. R.; Groeneman, R. H.; Atwood, J. L. *J. Am. Chem. Soc.* **1998**, *120*, 2676–2677.





**Figure 5.** Framework with van der Waals surface of the 2D host layer of **4** spreading over the *bc* plane. Benz[*a*]anthracene guests have been omitted for clarity. Color scheme: gray (carbon), white (hydrogen), blue (nitrogen), red (oxygen), yellow (sulfur), green (nickel). (b) Coordination environment around Ni(1), Ni(2), Ni(2)<sup>iii</sup> in **4** (50% probability level ellipsoids). Symmetry codes used to generate equivalent atoms: (i)  $-x, 1-y, 1-z$ ; (ii)  $x, y, -1+z$ ; (iii)  $-x, 1-y, -z$ .

**Table 5.** Selected Bond Distances (Å) and Angles (deg) for **4**<sup>a</sup>

Ni(1)–N(1)	2.057(2)	Ni(1)–N(11)	2.085(2)
Ni(1)–S(2)	2.5218(7)	Ni(2)–N(2)	2.020(2)
Ni(2)–N(3)	2.034(2)	Ni(2)–N(51) <sup>ii</sup>	2.118(2)
Ni(2)–N(31) <sup>i</sup>	2.123(2)	Ni(2)–S(1)	2.5146(8)
Ni(2)–S(3) <sup>iii</sup>	2.5601(8)		
N(1)–Ni(1)–N(11)	91.39(8)	N(1)–Ni(1)–S(2)	92.32(6)
N(11)–Ni(1)–S(2)	91.39(8)	N(2)–Ni(2)–N(31) <sup>i</sup>	91.17(9)
N(2)–Ni(2)–N(51) <sup>ii</sup>	93.74(9)	N(2)–Ni(2)–S(1)	90.62(6)
N(2)–Ni(2)–S(3) <sup>iii</sup>	81.99(6)	N(3)–Ni(2)–N(31) <sup>i</sup>	86.63(8)
N(3)–Ni(2)–N(51) <sup>ii</sup>	88.40(9)	N(3)–Ni(2)–S(1)	90.26(6)
N(3)–Ni(2)–S(3) <sup>iii</sup>	97.17(6)	N(31) <sup>i</sup> –Ni(2)–S(1)	91.13(6)
N(31) <sup>i</sup> –Ni(2)–S(3) <sup>iii</sup>	90.56(6)	N(51) <sup>ii</sup> –Ni(2)–S(1)	92.79(6)
N(51) <sup>ii</sup> –Ni(2)–S(3) <sup>iii</sup>	86.19(6)		

<sup>a</sup> Symmetry codes used to generate equivalent atoms: (i)  $-x, 1-y, 1-z$ ; (ii)  $x, y, -1+z$ ; (iii)  $-x, 1-y, -z$ .

**5**, respectively. The asymmetric unit contains two Ni<sup>2+</sup> ions (Ni(1) and Ni(2)) with octahedral coordination geometries, three SCN<sup>−</sup> ions, three pppeH ligands, and a benz[*a*]anthracene guest. Ni(1) lies on a crystallographic inversion center and Ni(2) does not. Figure 5b shows that the coordination environments around the metal centers are identical to those of **1–3**. One-dimensional chains consisting of Ni<sup>2+</sup> ions and  $\mu_{1,3}$ -intermetallic bridges of SCN<sup>−</sup> ions propagate along the *b* axis with Ni(1)/Ni(2) and Ni(2)/Ni(2)<sup>iii</sup> separations of 5.6029(3) and 5.5959(7) Å, respectively. Two pppeH ligands are bonded to the two axial coordination sites of each Ni<sup>2+</sup> ion via pyridyl nitrogen atoms. The bond lengths and angles of the coordination spheres of the Ni<sup>2+</sup> ions are compiled in Table 5. Each pppeH ligand forms a pppeH dimer with a pppeH ligand of an adjacent 1D chain through self-complementary pairwise O–H/O hydrogen bonding with O/O distances in the range 2.585(6)–2.64(2) Å, giving rise to the 2D host layer spreading over the *bc* plane.

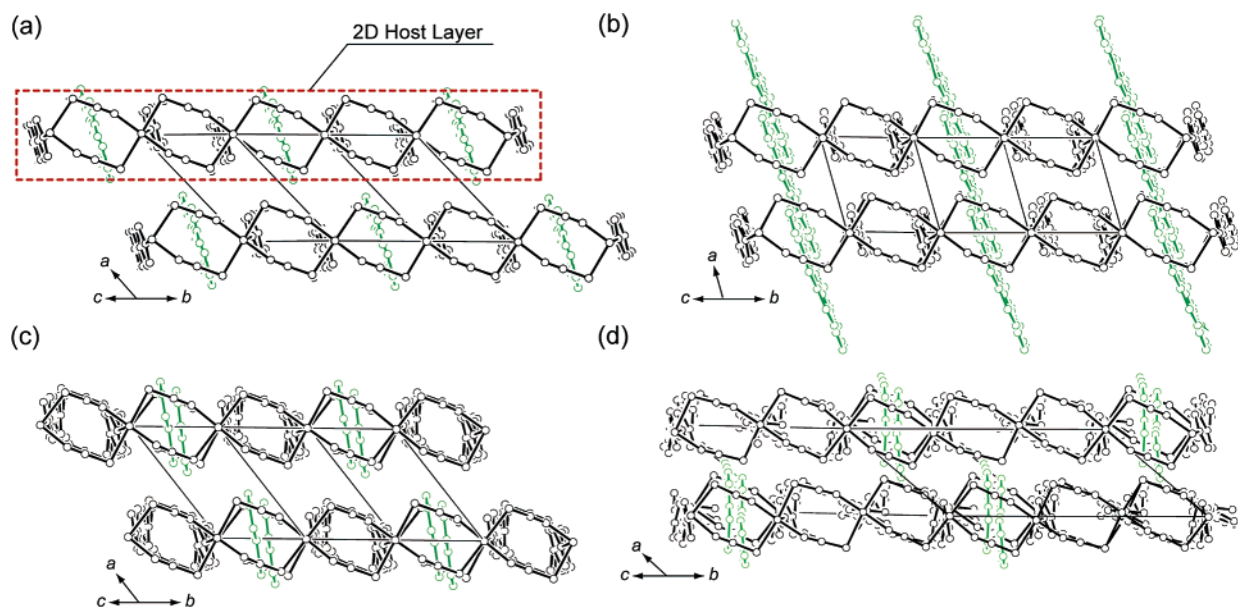
In contrast to **1–3**, two types of pppeH dimer were identified in the 2D host layers. Figure 5a shows that the one (pppeH dimer A) defines a boundary of a rectangular cavity and the other (pppeH dimer B) is sandwiched by two pppeH dimer A. The aromatic planes of pppeH dimer B are almost perpendicular (66.1–76.8°) to those of an adjacent pppeH dimer A. C–H/ $\pi$  interaction was identified between them. Its average distance (a distance between a hydrogen

atom of pppeH dimer B and a least-squares plane of an aromatic ring of adjacent pppeH dimer A) is 2.91 Å. Inter-chain Ni<sup>2+</sup>/Ni<sup>2+</sup> separations subjected by pppeH dimer A and pppeH dimer B are 29.521(1) and 29.728(1) Å, respectively. The latter is slightly longer than the former by 0.2 Å. The Ni<sup>2+</sup>–pppeH/pppeH–Ni<sup>2+</sup> linkages propagate along the [023] axis. Figure 5a shows that 2D host layers have RCs defined by two pppeH A dimers and two SCN bridges.

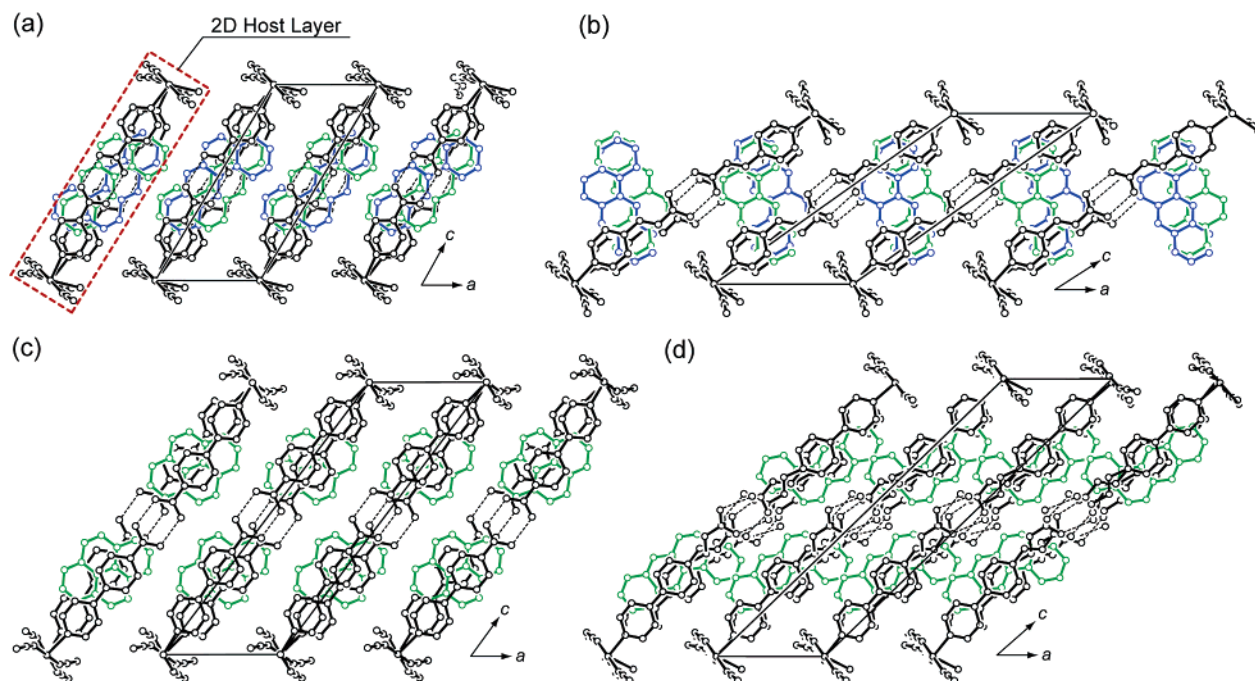
**Layered Structures.** The crystal structures viewed down along the [012] axis (**1–3**) and the [023] axis (**4**) are shown in Figure 6a–d, respectively. The 2D host layers of **1–4** are stacked parallel to the *bc* plane to give the layered structures. **1–4** are classified into two structural types according to relative locations between RCs of adjacent layers. The one is such that RCs of one layer are isolated from those of adjacent layers and the other is such that RCs of one layer adjoin those of adjacent layers to give 1D channels propagating along the stacking direction (*a* axis). **1, 3**, and **4** belong to the former type, and **2** belongs to the latter. Aromatic guests of either benz[*a*]anthracene (**1, 2, 4**) or pyrene (**3**) are included in RCs (**1, 3, 4**) or the 1D channels (**2**) with their aromatic planes parallel to those of the PCA dimers.

The crystal structures of **1–4** viewed down along the *b* axis are shown in Figure 7a–d, respectively. The 2D host layers are inclined by ca. 59° (**1**), 35° (**2**), 53° (**3**), and 44° (**4**) with respect to the *ab* planes of the respective crystal structures. Among them, 35° of **2** is substantially small compared to the others. As a result, the guest-accessible volume (GAV) of **2** is significantly reduced, regardless of the expansion of its potential GAV (vide infra).

Figure 7a–d shows the packing situations of aromatic guests in RCs (**1, 3, 4**) and in the 1D channel (**2**). In **1**, each RC contains one benz[*a*]anthracene guest. In **3** or **4**, each RC contains two pyrene or two benz[*a*]anthracene guests, respectively. In contrast, in **2**, each benz[*a*]anthracene guest penetrates two adjacent RCs such that the central moiety of a benz[*a*]anthracene guest is positioned between layers and its terminal moieties occupy the upper and the lower spaces of adjacent RCs. In **1** and **2**, the benz[*a*]anthracene guests



**Figure 6.** (a) Crystal structure of **1** viewed along the [012] axis. (b) Crystal structure of **2** viewed along the [012] axis. (c) Crystal structure of **3** viewed along the [012] axis. (d) Crystal structure of **4** viewed along the [023] axis. Hydrogen atoms are omitted for clarity.



**Figure 7.** Crystal structures of **1–4** viewed along the *b* axis. (a) Crystal structure of **1**. The benz[*a*]anthracene guests are disordered over two positions. (b) Crystal structure of **2**. The benz[*a*]anthracene guests are disordered over two positions. (c) Crystal structure of **3**. Each rectangular cavity contains two pyrene guests. (d) Crystal structure of **4**. Each rectangular cavity contains two benz[*a*]anthracene guests. Dotted lines show hydrogen bonds. Hydrogen atoms are omitted for clarity.

are disordered over two positions because they lie on crystallographic inversion centers.

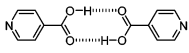
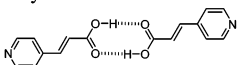
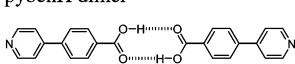
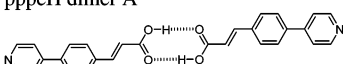
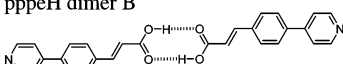

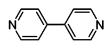
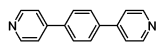
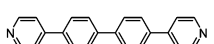
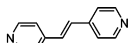
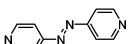
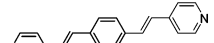
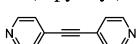

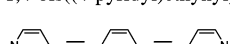
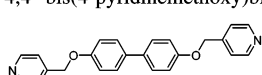
#### Structures of 4-Pyridyl-Substituted Carboxylic Acid Dimers

From the crystal structures of **1–4**, it is clear that the proposed structural extension is successful. In all cases, PCAs form the corresponding PCA dimers, acting as long bridging ligands. The lengths (interatomic distances between the pyridyl nitrogen atoms of the PCA dimers and the Ni/Ni separations subjected by them) of the PCA dimers and the Ni/Ni separations subjected by them are listed in Table 6 (entry 1–5). The lengths of the PCA dimers are

12.269(5) (isoH dimer), 16.890(4) (acrylH dimer), 20.89(4) (pybenH dimer), 25.387(3) (pppeH dimer A), and 25.527(4) Å (pppeH dimer B). The PCA dimers are elongated by almost twice the length of a hydrocarbon unit introduced between the pyridyl ring and the carboxyl functional group of each of three PCAs. The introduction of an ethenyl unit (from isoH to acrylH and from pybenH to pppeH) elongates the resulting bridging ligands by ca. 4.6 Å and that of a phenyl unit (from isoH to pybenH and from acrylH to pppeH) by ca. 8.5 Å. Of the three PCA dimers, pppeH dimer A and B (entry 4 and 5) amount to being twice as long as the isoH



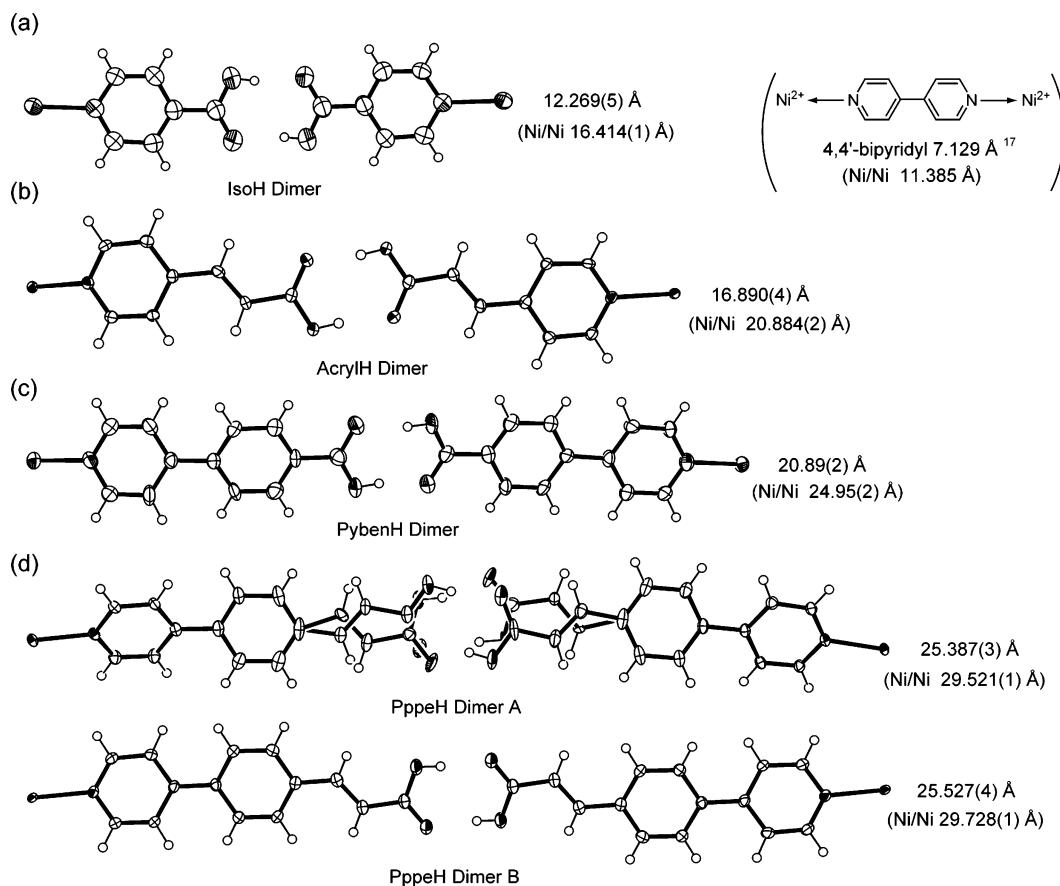
**Table 6.** Lengths (Å) and Metal–Metal Separations (Å) of the PCA Dimers and 4,4'-Bipyridine-Type Ligands<sup>a</sup>

entry	ligand	N/N (Å) <sup>b</sup>	metal/metal (Å) <sup>c</sup>	metal	ref.
1	isoH dimer 	12.269(5)	16.414(1)	Ni	–
2	acrylH dimer 	16.890(4)	20.884(2)	Ni	–
3	pybenH dimer 	20.89(2)	24.95(2)	Ni	–
4	pppeH dimer A 	25.387(3)	29.521(1)	Ni	–
5	pppeH dimer B 	25.527(4)	29.728(1)	Ni	–
6	pyradine 	2.823(10)	6.8178(18)	Cu	16
7	4,4'-bipyridine 	7.129(6)	11.3853(12)	Ni	17
8	1,4-bis(4-pyridyl)benzene 	11.398(3)	15.229(4)	Ni	18
9	4,4'-bis(4-pyridyl)biphenyl 	15.756(3)	19.9214(16)	Ni	18
10	trans-1,2-bis(4-pyridyl)ethylene 	9.344(11)	13.2560(18)	Cu	16
11	trans-4,4'-azobipyridine 	9.011(5)	12.9906(16)	Cu	16
12	trans,trans-1,4-bis(2-(4-pyridyl)ethenyl)benzene 	16.097(7)	– <sup>d</sup>	Co	19
13	bis(4-pyridyl)acetylene 	9.657(4)	14.404(2)	Cd	20
14	bis(4-pyridyl)butadiyne 	12.212(5)	16.759(2)	Mn	21
15	1,4-bis((4-pyridyl)ethynyl)benzene 	16.516(4)	20.7828(16)	Co	22
16	4,4'-bis(4-pyridinemethoxy)biphenyl 	19.776(18)	23.779(15)	Co	19

<sup>a</sup> Lengths (Å) and metal–metal separations (Å) of 4,4'-bipyridine-type ligands were calculated by the *PLATON* program package. See ref 27. <sup>b</sup> An interatomic distance (Å) between the pyridyl nitrogen atoms of a bridging ligand. <sup>c</sup> An interatomic distance (Å) between the metal centers linked by a bridging ligand. <sup>d</sup> *trans,trans*-1,4-Bis(2-(4-pyridyl)ethenyl)benzene acts as a monodentate ligand.

dimer (entry 1). The Ni/Ni separations are also elongated with the elongation of the PCA dimers. The Ni/Ni separations are 16.414(1) (isoH dimer), 20.884(2) (acrylH dimer), 24.95(2) (pybenH dimer), 29.521(1) (pppeH dimer A), and 29.728(1) Å (pppeH dimer B). The Ni/Ni separations of the latter two amount to 30 Å.

Figures 8 and S5 (see the Supporting Information) show the front and side views of the PCA dimers found in **1–4**, respectively. The isoH and the acrylH dimers adopt a slightly twisted arrangement of their constituent hydrocarbon units: the dihedral angles between the pyridyl rings and the central R<sub>2</sub>(8) ring systems are 3.7(2) and 11.7(2)° for the isoH



**Figure 8.** ORTEP drawing of the front views of the PCA dimers formed in **1–4** (50% probability level ellipsoid): (a) isoH dimer; (b) acrylH dimer; (c) pybenH dimer; (d) pppeH dimer A and B. The central moiety of pppeH dimer A is disordered over two positions. The site occupancy factor of its major component is 0.744(6) at 153 K.

dimer and  $5.2(2)$  and  $16.8(2)^\circ$  for the acrylH dimer. The pybenH and the pppeH dimers adopt twisted structures about  $C_{\text{pyridyl}}-C_{\text{phenyl}}$  bonds, originating from steric repulsion between hydrogen atoms on the ortho carbon atoms of adjacent rings: the corresponding dihedral angles are  $14.1(3)$  and  $25.1(3)^\circ$  for the pybenH dimer,  $23.5(1)$  and  $21.0(1)^\circ$  for pppeH dimer A, and  $21.7(3)^\circ$  for pppeH dimer B. The central moieties of the pybenH and pppeH dimers (the phenyl-CO<sub>2</sub>H/CO<sub>2</sub>H-phenyl moiety of the pybenH dimer and the phenylethenyl-CO<sub>2</sub>H/CO<sub>2</sub>H-phenylethenyl moieties of the pppeH dimers) adopt slightly twisted structures: the dihedral angles between the phenyl rings and the central  $R_2^2(8)$  ring systems are almost identical to those observed in the previous two PCA dimers.

The lengths of 4,4'-bipyridine-type ligands employed in metal-organic coordination frameworks and metal/metal separations subjected by them are listed in Table 6 (entry 6–16). At a first glance, the pybenH and pppeH dimers are substantially long bridging ligands compared with the 4,4'-bipyridine-type ligands. The pppeH dimers (entry 4 and 5), which are the longest PCA dimers reported herein, are three-and-a-half times as long as a 4,4'-bipyridine ligand<sup>17</sup> ( $7.129(6)$  Å) (entry 7), which is in the most widespread use in metal-organic coordination frameworks<sup>15,17,23</sup> and other supramolecular systems<sup>24</sup>, and are much longer than the 4,4'-bis(4-pyridylmethoxy)biphenyl ligand<sup>22</sup> ( $19.776(18)$  Å; entry

16). The latter one is a very long 4,4'-bipyridine-type ligand almost 20 Å in length and is much longer than most of the 4,4'-bipyridine-type ligands reported to date. To the best of our knowledge, the pppeH dimer is one of the longest bridging ligands employed in the metal-organic coordination framework. The pybenH dimer (entry 3), which is shorter than the pppeH dimers by ca. 4.6 Å (entry 4 and 5), is comparable to this very long 4,4'-bipyridine-type ligand. Although the acrylH dimer is the shortest PCA dimer of the three (entry 2), it bears favorable comparison with the 4,4'-bis(4-pyridyl)biphenyl<sup>18</sup> ( $15.756(3)$  Å; entry 9), *trans,trans*-1,4-bis(2-(4-pyridyl)ethenyl)benzene<sup>19</sup> ( $16.097(7)$  Å; entry 12), and 1,4-bis(4-pyridylethynyl)benzene<sup>22</sup> ( $16.516(4)$  Å; entry 15) ligands. In addition to these three PCA dimers, the isoH dimer (entry 1), the fundamental PCA dimer, is comparable to the 1,4-bis(4-pyridyl)benzene<sup>18</sup> ( $11.398(3)$  Å; entry 8) and bis(4-pyridyl)butadiyne<sup>21</sup> ( $12.212(5)$  Å; entry

(16) Carlucci, L.; Ciani, G.; Gramaccioli, A.; Proserpio, D. M.; Rizzato, S. *CrystEngComm* **2000**, *29*, 1–10.

(17) Biradha, K.; Domasevitch, K. V.; Moulton, B.; Seward, C.; Zaworotko, M. J. *Chem. Commun.* **1999**, 1327–1328.

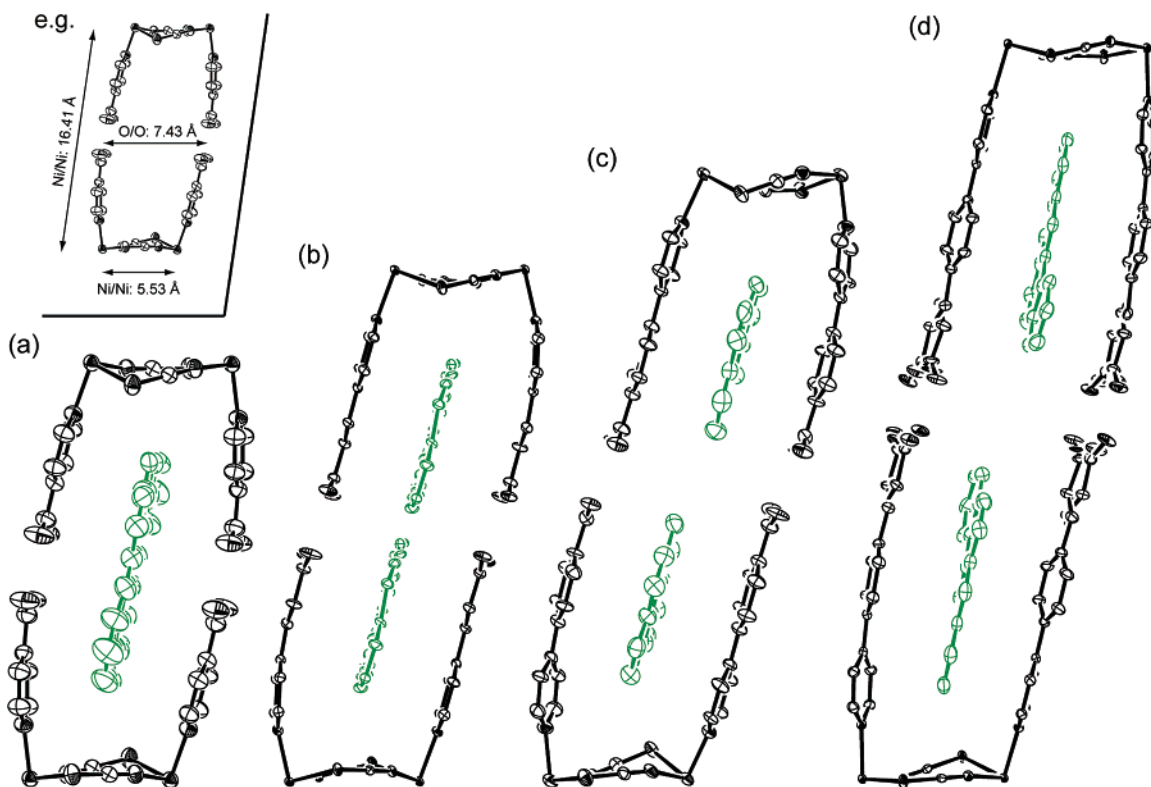
(18) Biradha, K.; Fujita, M. *Chem. Commun.* **2001**, 15–16.

(19) Banfi, Stefano.; Carlucci, L.; Caruso, E.; Ciani, G.; Proserpio, D. M. *J. Chem. Soc., Dalton Trans.* **2002**, 2714–2721.

(20) Dong, Y.-B.; Layland, R. C.; Smith, M. D.; Pscirer, N. G.; Bunz, U. H. F.; Loye, H.-C. *Inorg. Chem.* **1999**, *38*, 3056–3060.

(21) Zaman, M. B.; Udachin, K. A.; Ripmeester, J. A. *CrystEngComm* **2002**, *4*, 613–617.

(22) Zaman, M. B.; Udachin, K.; Ripmeester, J. A.; Smith, M. D.; Loye, H.-C. *Inorg. Chem.* **2005**, *44*, 5047–4059.



**Figure 9.** ORTEP drawing of the front views of the rectangular cavities formed in **1–4** (50% probability level ellipsoid): (a) rectangular cavity of **1** ( $16.41 \times 5.53\text{--}7.43 \text{ \AA}^2$ ); (b) rectangular cavity of **2** ( $20.88 \times 5.49\text{--}7.25 \text{ \AA}^2$ ); (c) rectangular cavity of **3** ( $24.95 \times 5.46\text{--}7.38 \text{ \AA}^2$ ); (d) rectangular cavity of **4** ( $29.52 \times 5.60\text{--}7.20 \text{ \AA}^2$ ). Hydrogen atoms are omitted for clarity.

14) ligands. These comparisons exemplify that the design strategy, the preparation of bridging ligands through self-assembly of two PCAs with the assistance of CAD formation, is both efficient and particularly suitable for the preparation of very long bridging ligands.

Easy preparation of the PCA dimers is also a notable feature of this design strategy. The PCA dimers consist of two corresponding PCAs which are either commercially available (isoH and acrylH) or synthesized in one (pybenH) or two steps (pppeH). Despite their easy preparation, the resulting PCA dimers act as very long bridging ligands, some of which are well more than 20 Å in length. These two features, that is, their considerable lengths and easy preparation, are advantageous over their single molecular counterparts in the construction of metal–organic coordination frameworks.

Interestingly, the ethenyl units and the central  $R_2^2(8)$  ring system of the pppeH dimer A is disordered over two positions. The site occupancy factor of its major component is 0.744(6) at 153 K. This disorder might indicate that the central moiety of pppeH dimer A, that is, the ethenyl– $\text{CO}_2\text{H}$ /CO<sub>2</sub>H–ethenyl moiety, undergoes a rotation like the pedal motion of a bicycle.<sup>25</sup> This type of dynamic disorder in the

crystalline state has been reported by several groups<sup>26</sup>. Detailed analysis will be reported elsewhere. On the other hand, no such disorder was identified in pppeH dimer B. Most likely, the C–H/ $\pi$  interaction between pppeH dimer B and pppeH dimer A fixes its orientation.

**Structures of The Rectangular Cavities.** The elongation of the bridging ligands successfully expanded the cavity dimensions of **2–4** without the formation of an interpenetrating network. Figure 9 shows that the architectures of RCs formed in **1–4** are very similar to each other. They have spindle-like shapes. The widths of RCs vary from ca. 5.53 (**1**), 5.49 (**2**), 5.46 (**3**), and 5.60 Å (**4**) (these values are in agreement with the Ni/Ni separations subjected by the SCN bridges) to ca. 7.43 (**1**), 7.25 (**2**), 7.38 (**3**), and 7.20 Å (**4**) (these values are in agreement with O/O distances between the PCA dimers). The heights of RCs are ca. 16.41 (**1**), 20.99 (**2**), 24.95 (**3**), and 29.52 Å (**4**), which are in agreement with the Ni/Ni separations subjected by the respective PCA dimers. Therefore, the cavity dimensions of **1–4** are  $16.41 \times 5.53\text{--}7.43$ ,  $20.88 \times 5.49\text{--}7.25$ ,  $24.95 \times 5.46\text{--}7.38$ , and  $29.52 \times 5.60\text{--}7.20 \text{ \AA}^2$ , respectively.

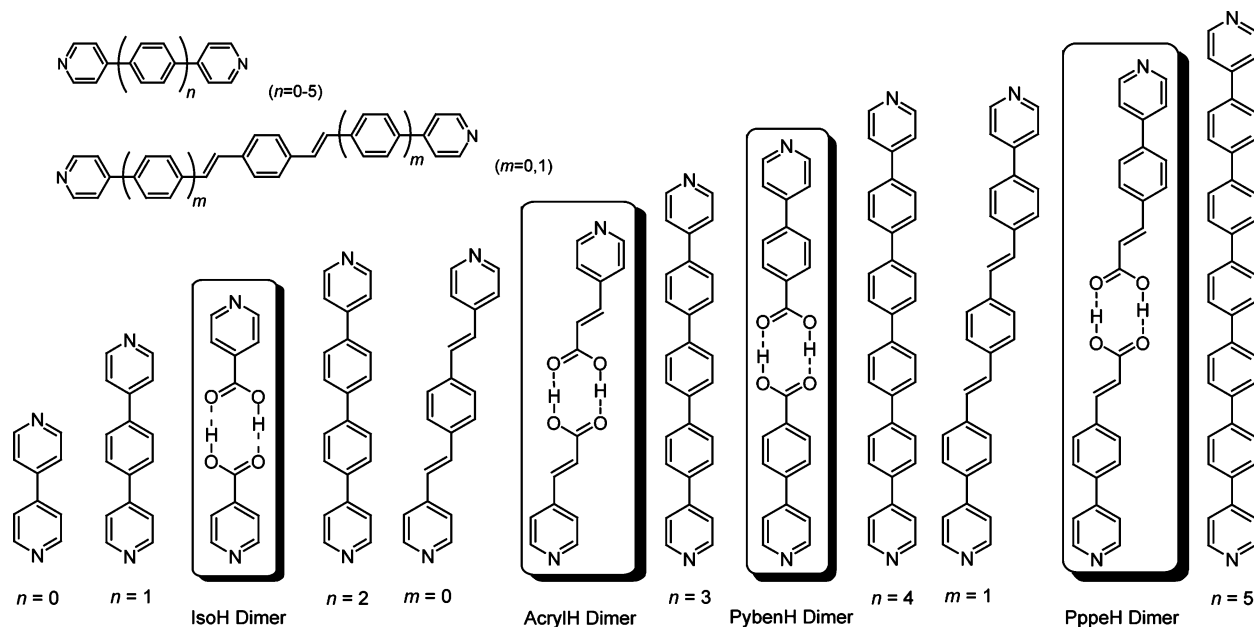
(23) For recent articles (metal–organic coordination frameworks) see: (a) Ohmori, O.; Fujita, M. *Chem. Commun.* **2004**, 1586–1587. (b) Kitaura, R.; Seki, K.; Akiyama, G.; Kitagawa, S. *Angew. Chem., Int. Ed.* **2003**, *42*, 428–431. (c) Noro, S.; Kitagawa, S.; Kondo, M.; Seki, K. *Angew. Chem., Int. Ed.* **2000**, *39*, 2081–2084. (d) Subramanian, S.; Zaworotko, M. J. *Angew. Chem., Int. Ed.* **1995**, *34*, 2127–2129. (e) Fujita, M.; Kwon, Y. J.; Washizu, S.; Ogura, K. *J. Am. Chem. Soc.* **1994**, *116*, 1151–1152.

(24) For recent articles (pure organic systems) see: (a) Varughese, S.; Pedireddi, V. R. *Chem.–Eur. J.* **2006**, *12*, 1597–1609. (b) Santis, A.; Formi, A.; Liantonio, R.; Metrangolo, P.; Pilati, T.; Resnati, G. *Chem.–Eur. J.* **2003**, *9*, 3974–3983. (c) MacGillivray, L. R.; Reid, J. L.; Ripmeester, J. A. *Chem. Commun.* **2001**, 1034–1034.

(25) (a) Harada, J.; Ogawa, K. *J. Am. Chem. Soc.* **2001**, *123*, 10884–10888. (b) Harada, J.; Ogawa, K.; Tomoda, S. *Acta Crystallogr., Sect. B.* **1997**, *53*, 662–672.

(26) (a) Ohba, S.; Hosomi, H.; Ito, T. *J. Am. Chem. Soc.* **2001**, *123*, 6349–6352. (b) Natarajan, A.; Mague, J.T.; Venkatesan, K.; Ramamurthy, V. *Org. Lett.* **2005**, *7*, 1895–1898.





**Figure 10.** Molecular structures of the four PCA dimers, bipy, and its analogues ( $n = 0-5$ ,  $m = 0, 1$ ).

GAVs of **1-4** calculated by the *PLATON* program package<sup>27</sup> are 390.6, 380.7, 663.6, and 743.0 Å<sup>3</sup>, respectively. In comparison to GAV of **1**, GAVs of **3** and **4** are expanded by 273 and 352 Å<sup>3</sup>, respectively. In particular, 743.0 Å<sup>3</sup> of **4** amounts to being about twice as large as 390.6 Å<sup>3</sup> of **1**. The fact that GAV of **2** is the smallest one of the four has a close relation with its crystal structure. As mentioned above, the 2D host layers are inclined by ca. 34.5° with respect to the *ab* plane, so that the upper and the lower spaces of RCs of one layer are partly preoccupied by the 1D chains of adjacent layers. As a result, GAV of **2** becomes small regardless of the expansion of its potential GAV.

The expansion successfully increases the number of guests that can be included in RCs. The RC of **1** contains only one molecule of benz[*a*]anthracene, whereas the RC of **3** or **4** contains two molecules of pyrene or benz[*a*]anthracene, respectively. These results indicate that aromatic guests whose sizes are, in principle, up to twice as large as pyrene or benz[*a*]anthracene should be included in the RC of **3** or **4**, respectively. A detailed survey of inclusion properties is currently in progress.

#### 4-Pyridyl-Substituted Carboxylic Acid Dimers: Supramolecular Analogues of 4,4'-Bipyridine-Type Ligands.

From the structures of the PCA dimers found in **1-4**, it is evident that they can be regarded as being supramolecular analogues of 4,4'-bipyridine-type ligands. Figure 10 shows the molecular structures of the four PCA dimers, bipy, and its analogues ( $n = 1-5$ ,  $m = 0, 1$ ). Considering the lengths of the PCA dimers, the isoH, acrylH, pybenH, and pppeH dimers are supramolecular analogues of 1,4-bis(4-pyridyl)-benzene ( $n = 1$ ), *trans,trans*-1,4-bis(2-(4-pyridyl)ethenyl)-benzene (and 4,4'-bis(4-pyridyl)biphenyl ( $n = 2$ )), 4,4''-bis(4-pyridyl)-*p*-terphenyl ( $n = 3$ ), and *trans,trans*-1,4-bis(2-(4-(4-pyridyl)phenyl)ethenyl)benzene (and 4,4'''-bis(4-pyridyl)-

quaterphenyl ( $n = 4$ )), respectively. The three former ligands have been employed in metal-organic coordination frameworks,<sup>20,21,25,26</sup> whereas the three latter have not. This is probably closely related to their solubility toward solvents. On the other hand, the pybenH dimer and the pppeH dimers could be employed as bridging ligands of the metal-organic coordination frameworks despite their lengths of well more than 20 Å. This is because they are not single molecules but consist of two corresponding PCAs.

#### Conclusion

In conclusion, the proposed structural extension was successful. These expansion increases the number of aromatic guests that can be included in the rectangular cavities (RCs) from one molecule of benz[*a*]anthracene (**1**) to two molecules of pyrene (**3**) or benz[*a*]anthracene (**4**). The 4-pyridyl-substituted carboxylic acid (PCA) dimers can be regarded as being supramolecular analogues of 4,4'-bipyridine-type ligands because of their structural equivalence. Comparison of the lengths between the PCA dimers and 4,4'-bipyridine-type ligands demonstrated that a design strategy, that is, the preparation of a bridging ligands though self-assembly of two PCAs with assistance of carboxylic acid dimer formation, is both efficient and particularly suitable for the preparation of very long bridging ligands.

**Acknowledgment.** We are grateful to professor Matsushita for permission to use a Rigaku RAXIS-RAPID imaging plate area detector. This work was supported by a Grant-in-Aid for Scientific Research (17750122) from the Ministry of Education, Culture, Sports, Science, and Technology of Japan.

**Supporting Information Available:** X-ray crystallographic data in CIF format for **1-4**; IR spectra of **1-4**; side views of the PCA dimers (PDF). This material is available free of charge via Internet at <http://pubs.acs.org>.

(27) Spek, A. L. *PLATON*; University of Glasgow: Glasgow, Scotland, 1998.